



Title	Solvothermal syntheses of semiconductor photocatalysts of ultra-high activities
Author(s)	Kominami, Hiroshi; Kato, Jun-ichi; Murakami, Shin-ya et al.
Description	<p>Thermal treatment of titanium(IV) butoxide dissolved in 2-butanol at 573 K under autogenous pressure (alcoholthermal treatment) yielded microcrystalline anatase-type titanium(IV) oxide (TiO₂). Thermal treatment of oxobis(2,4-pentanedionato-0,0')titanium (TiO(acac)₂) in ethylene glycol (EG) in the presence of sodium acetate and a small amount of water at 573 K yielded microcrystalline brookite-type TiO₂. Tungsten(VI) oxide (WO₃) powders of monoclinic crystal structure with high crystallinity were synthesized by hydrothermal treatment (HTT), at 523 or 573 K, of aqueous tungstic acid (H₂WO₄) solutions prepared from sodium tungstate by ion-exchange (IE) with a proton-type resin. Anatase and brookite TiO₂ products were calcined at various temperatures and then used for photocatalytic mineralization of acetic acid in aqueous solutions under aerated conditions and dehydrogenation of 2-propanol under deaerated conditions. Almost all the anatase-type TiO₂ samples showed the activities more than twice higher than those of representative active photocatalysts, Degussa P-25 and Ishihara ST-01 in both reactions. A brookite sample with improved crystallinity and sufficient surface area obtained by calcination at 973 K exhibited the hydrogen evolution rate almost equal to P-25. HTT WO₃ powders with various physical properties were used as photocatalyst for evolution of oxygen (O₂) from an aqueous silver sulfate solution. WO₃ powder of high crystallinity, e.g., IE-HTT-WO₃ synthesized at 573 K, gave much higher O₂ yield than commercially available WO₃ samples.</p> <p>http://www.elsevier.com/wps/find/journaldescription.cws_home/500857/description</p>
Citation	Catalysis Today, 84(3-4), 181-189 https://doi.org/10.1016/S0920-5861(03)00272-4
Issue Date	2003-09-15
Doc URL	https://hdl.handle.net/2115/17127
Type	journal article
File Information	CT84-3-4.pdf



Solvothermal Syntheses of Semiconductor Photocatalysts of Ultra-high Activities

Hiroshi Kominami, Jun-ichi Kato, Shin-ya Murakami, Yoshinori Ishii, Masaaki Kohno, Kei-ichi Yabutani, Takuhei Yamamoto, Yoshiya Kera, Masashi Inoue,^a Tomoyuki Inui,^a Bunsho Ohtani^b

Department of Applied Chemistry, Faculty of Science and Engineering, Kinki University, Kowakae, Higashiosaka, Osaka 577-8502, Japan

^aDepartment of Energy and Hydrocarbon Chemistry, Graduate School of Engineering, Kyoto University, Yoshida, Kyoto 606-8501, Japan

^bCatalysis Research Center, Hokkaido University, Sapporo 060-0811, Japan.

Abstract

Thermal treatment of titanium(IV) butoxide dissolved in 2-butanol at 573 K under autogenous pressure (alcoholothermal treatment) yielded microcrystalline anatase-type titanium(IV) oxide (TiO₂). Thermal treatment of oxobis(2,4-pentanedionato-O,O')titanium (TiO(acac)₂) in ethylene glycol (EG) in the presence of sodium acetate and a small amount of water at 573 K yielded microcrystalline brookite-type TiO₂. Tungsten(VI) oxide (WO₃) powders of monoclinic crystal structure with high crystallinity were synthesized by hydrothermal treatment (HTT), at 523 or 573 K, of aqueous tungstic acid (H₂WO₄) solutions prepared from sodium tungstate by ion-exchange (IE) with a proton-type resin. Anatase and brookite TiO₂ products were calcined at various temperatures and then used for photocatalytic mineralization of acetic acid in aqueous solutions under aerated conditions and dehydrogenation of 2-propanol under deaerated conditions. Almost all the anatase-type TiO₂ samples showed the activities more than twice higher than those of representative active

photocatalysts, Degussa P-25 and Ishihara ST-01 in both reactions. A brookite sample with improved crystallinity and sufficient surface area obtained by calcination at 973 K exhibited the hydrogen evolution rate almost equal to P-25. HTT WO_3 powders with various physical properties were used as photocatalyst for evolution of oxygen (O_2) from an aqueous silver sulfate solution. WO_3 powder of high crystallinity, e.g., IE-HTT- WO_3 synthesized at 573 K, gave much higher O_2 yield than commercially-available WO_3 samples

1. INTRODUCTION

Titanium(IV) oxide (TiO_2) has attracted much attention mainly in expectation of being applied to environmental photocatalytic processes such as deodorization, prevention of stains, sterilization [1], and removal of pollutants from air and water [2-4]. For the realization of their practical application, development of highly active TiO_2 photocatalyst is keenly desired. Based on the kinetic investigation of photocatalytic reactions, we have pointed out that TiO_2 particles having both large surface area and high crystallinity must exhibit higher photocatalytic activity [5]. The former property should increase the amount of surface-adsorbed substrate(s) to enhance the capture of photogenerated electron (e^-) and positive hole (h^+), and the latter, i.e., less defects acting as the recombination center, should suppress mutual e^- - h^+ recombination. However, it is generally difficult to satisfy these two properties by representative methods such as precipitation and sol-gel technique.

Among TiO_2 there exist three crystal phases; anatase, rutile and brookite. The anatase and rutile phases are well known and many studies on their synthesis, photocatalysis and application for catalyst supports have been reported. On the other hand, only a few studies on the synthesis of brookite-type TiO_2 have been examined [6,7]. To our knowledge, there is only one paper in which synthesized brookite TiO_2 was successfully used as catalyst materials [8]. Difficulty to prepare brookite having both high purity and large surface is

probably one of the reasons for limited application of brookite TiO_2 as catalyst support and photocatalyst.

Tungsten(VI) oxide (WO_3), whose band gap energy has been estimated to be 2.5 eV, has the potential ability to photocatalyze under irradiation of visible light of wavelength $<$ ca. 500 nm. Actually, visible light-induced action of oxidizing water has been reported using WO_3 powder and iron(III) ions (or silver ions) as the electron acceptor [9-12]. However, commercially available WO_3 powders have been used in these studies, and the properties of WO_3 suitable for the photocatalytic activity for oxygen (O_2) evolution have not been clarified. The photocatalytic O_2 evolution, a half part of stoichiometric water decomposition, seem still ambiguous in its mechanism and, thereby, investigations on the visible light-induced evolution on WO_3 are needed for, e.g, development of solar energy conversion systems.

In this study, we applied solvothelmal method to synthesize semiconductor photocatalysts of high activities. When water (H_2O) is used as the synthesis medium, the method is called hydrothelmal method [13]. Similarly, alcohothermal means solvothelmal in alcohol [14]. Here, we show solvothelmal syntheses of three photocatalysts, alcohothermal synthesis of anatase-type TiO_2 , solvothelmal synthesis of brookite-type TiO_2 in glycol- H_2O medium, and hydrothelmal synthesis of WO_3 .

2. EXPERIMENTAL

2.1 Alcohothermal synthesis of anatase-type TiO_2

Titanium(IV) alkoxides, 10 g, was dissolved in a 70 cm^3 portion of an alcohol in a test tube which was then set in a 200-cm^3 autoclave (Figure 1). An additional 30 cm^3 of the alcohol was placed in the gap between the test tube and the autoclave wall. The autoclave was thoroughly purged with nitrogen, heated to desired temperature (523-573 K) at a rate of 2.5 K min^{-1} , and kept at that temperature for 2 h. After the autoclave treatment, the

resulting powders were washed repeatedly with acetone and dried in air.

2.2 Synthesis of brookite-type TiO₂ in glycol-water medium

Typical synthesis procedure is as follows [15]: Oxobis(2,4-pentanedionato-O,O')titanium (TiO(acac)₂, 0.019 mol) (Tokyo Kasei) and sodium acetate (0.038 mol) (Kanto Chemical) were added to 70 cm³ of ethylene glycol (EG) (Kanto Chemical) in a test tube, which was then set in 200 cm³ autoclave. In the gap between the test tube and the autoclave wall, 5 cm³ of water was added. At this point, water contacted neither TiO(acac)₂ nor EG. The autoclave was purged with nitrogen, heated at 573 K at a rate of 2.5 K min⁻¹, and held at that temperature for 2 h. During the reaction, water was vaporized and dissolved in EG. The products were washed first with acetone and then with water repeatedly under sonication, and dried at room temperature.

2.3 Hydrothermal synthesis of WO₃

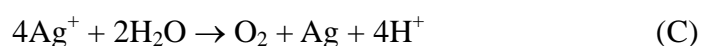
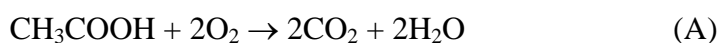
Aqueous H₂WO₄ solutions were prepared by the cation-exchange method with a strongly acidic ion-exchange (IE) resin in its proton (H⁺) form [16]. Prior to IE, diluted hydrochloric acid (HCl) (0.1 mol dm⁻³, 240 cm³) was added to the resin (Organo, Amberlite IR120B NA, 30 cm³) packed in a glass column to make it in the H⁺ form and then the resin was washed with distilled water until chloride ions were no longer detected in the eluent. An aqueous solution of NaWO₄ (Wako; 0.39 mol dm⁻³, 37.5 cm³) was loaded on the column and H₂WO₄ was recovered from the column by elution with distilled water (37.5 cm³). The concentration of H₂WO₄ solution in the elute (75 cm³) was determined to be 0.19 mol dm⁻³, which corresponded to 98 % recovery.

The clear H₂WO₄ solution in the glass tube was set in a 300-cm³ autoclave. The gap between the tube and inside wall of the autoclave was filled with 25 cm³ of water. The

autoclave was thoroughly purged with nitrogen, heated to a desired temperature (473-573 K) at a rate of 2.5 K min⁻¹, and kept at that temperature for 2 h. After the heating, the resulting powder was washed repeatedly with acetone and dried in air at room temperature. Hydrothermal treatment (HTT) of solid H₂WO₄ with tungstite structure (supplied as “tungstic acid” from Kanto Chemicals) was also carried out under conditions similar to those described above.

2.4 Calcination and characterization

Calcination of the samples was carried out in a box furnace; the sample in a combustion boat was heated to the desired temperature at a rate of 10 K min⁻¹ and kept at that temperature for 1 h. Powder X-ray diffraction (XRD) with CuK α radiation was recorded on a Rigaku RINT 2500 diffractometer equipped with a carbon monochromator. Thermogravimetry (TG) and differential thermal analysis (DTA) were performed using a Rigaku TG-8120 under a flow of air at 100 cm³ min⁻¹. Morphology of the powders was observed using a JEOL 5200 scanning electron microscope (SEM) and a JEOL JEM-3010 transmission electron microscope (TEM). Diffuse reflectance spectra were obtained by a Shimadzu UV-2400 UV-vis spectrometer equipped with a diffuse reflectance measurement unit (ISR-2000) and recorded after Kubelka-Munk analysis. Specific surface area was determined by the BET single-point method using nitrogen uptake at 77 K.



2.5 Photoirradiation and product analyses

(A) Photocatalytic reaction in an aqueous AcOH solution: bare TiO₂ powder (50 mg) was suspended in an AcOH solution (175 μmol, 5.0 cm³) [17]. (B) Photocatalytic reaction in an aqueous 2-PrOH solution: Pt (0.1 wt%)-TiO₂ powder (50 mg) was suspended in a 2-PrOH solution (500 μmol, 5.0 cm³) [18]. (C) Photocatalytic reaction in an aqueous silver sulfate (Ag₂SO₄) solution: bare TiO₂ powder (50 mg) was suspended in an Ag₂SO₄ solution (125 μmol, 5.0 cm³) [19]. The reaction of (A) was carried out in reaction tubes (18 mm in diameter and 180 mm in length, transparent for light with a wavelength of > 300 nm) under aerated conditions, while those of (B) and (C) was carried out under an Ar atmosphere. The suspension was stirred (1000 rpm) at 298 K by using a magnet bar. After the irradiation, the amounts of carbon dioxide (CO₂), hydrogen (H₂) and O₂ in the gas phase of reaction mixtures were measured using a Shimadzu GC-8A gas chromatograph equipped with Porapak QS (CO₂) and MS-5A (H₂ and O₂) columns. The amounts of 2-PrOH and acetone were analyzed using a Shimadzu GC-8A gas chromatograph equipped with an FID and a column packed with PEG20M. Deposited Ag was analyzed by inductively coupled plasma emission spectroscopy (ICP, Shimadzu ICPS-1000III) after dissolution with concentrated nitric acid (HNO₃).

3. Results and Discussion

3.1 Characterization of TiO₂ prepared by alcohothermal method

An XRD pattern of the product prepared by alcohothermal treatment of titanium n-butoxide (TNB) in 2-butanol at 573 K is depicted in Figure 2(a), which shows that anatase [20] was formed without contamination of any other phases such as rutile or brookite. Addition of water to the supernatant after the autoclaving gave no precipitates, indicating that TNB was completely hydrolyzed during the thermal treatment. Judging from the fact that the treatment of TNB in toluene at the same temperature yielded no product, the source of

water for the hydrolysis was that generated from 2-butanol. This sample possessed sufficient surface area of $63 \text{ m}^2\text{g}^{-1}$ and the crystallite size of this sample was calculated to be 19 nm from the line-broadening of the 101 diffraction peak of anatase. TEM observation (Figure 3) revealed that the sample consisted of the agglomerates of primary particles of an average diameter of 20 nm, which was in good agreement with the crystallite size estimated from the XRD pattern. Therefore, each particle observed in TEM should be a single anatase crystal. TG analysis revealed that this sample showed gradual weight loss of 2.42% from 373 to 1273 K and only a very weak exothermic peak at 560 K was observed in a DTA curve due to combustion of a small amount of remaining organic moieties. Absence of sharp exothermic peak due to crystallization of anatase at around 673-773 K suggests that the product contains a negligible amount of amorphous-like phase, which is well consistent with the results of XRD and TEM. When titanium isopropoxide (TIP) was dissolved in a mixed solvent of 7 vol% 2-propanol in toluene, TIP was completely hydrolyzed to give anatase as observed in 100% 2-propanol. The amount of water required for complete hydrolysis of TIP is calculated to be 0.14 mol. Assuming that 2-propanol in toluene is completely dehydrated, the amount of water formed from the mixed solvent is estimated to be 0.064 mol, which is smaller than that necessary for the complete hydrolysis of TIP. Two possibilities might account for this; 2-propanol formed by hydrolysis of TIP was dehydrated to yield water which was then used for the hydrolysis, and/or water generated by dehydration of hydrated TiO_2 was used again to hydrolyze TIP. In both processes water was recycled. In the present paper, the TiO_2 sample prepared by alcohothermal method is called THyCA (Transfer Hydrolytic Crystallization in Alcohols) TiO_2 .

Effect of calcination on physical properties of THyCA- TiO_2 prepared in the TNB-2-butanol system is shown in Figure 4. Post-calcination at temperatures lower than 973 K reduced the BET surface area slightly. This is consistent with the result that the

XRD pattern of the TiO₂ sample calcined at 823 K was almost identical to that before calcination, as shown in Figure 2(b). Even after calcination at 973 K, the THyCA-TiO₂ was composed of small anatase crystallite of 26 nm diameter (Figure 2(c)) and still possessed sufficient surface area of 45 m²g⁻¹. Calcination at 1173 K induced partial transformation into the rutile, but the sample still predominantly consisted of the anatase crystallite (Figure 2(d)). The high thermal stability of THyCA-TiO₂ is interpreted by assuming that the as-prepared THyCA TiO₂ consists of single crystals and contains negligible amount of amorphous-like phase to be crystallized into anatase and to induce sintering of crystallites upon calcination.

3.2 Photocatalytic activities of THyCA-TiO₂

Figure 5 shows the effect of calcination on the CO₂ evolution rate of THyCA-TiO₂ in photocatalytic mineralization of acetic acid. Uncalcined THyCA-TiO₂ exhibited the rate of 21.3 μmol h⁻¹ that was much larger than those of representative commercial TiO₂, Degussa P-25 and Ishihara ST-01 (8.5 and 11.6 μmol h⁻¹), which have been known to show high photocatalytic activity. Since the THyCA-TiO₂ powders satisfied the basic requirements for active TiO₂ photocatalyst, i.e., both large surface area and sufficient crystallinity, the present results can be reasonably accepted. An amorphous hydrated TiO₂ of quite large surface area prepared by hydrolysis under atmospheric conditions showed negligible activity (<1 μmol h⁻¹), due to large recombination probability of photogenerated e⁻ and h⁺ at large number of surface defects. Calcination of THyCA-TiO₂ powders decreased their photocatalytic activities, suggesting that surface area, i.e., adsorptivity to toward acetic acid, is decisive factor in this reaction system.

Effect of calcination on the H₂ evolution rate of platinized THyCA-TiO₂ in photocatalytic dehydrogenation of 2-propanol in aqueous suspension is shown in Figure 6.

It should be noted that temperature dependency of the rate was different from that of mineralization of acetic acid. The rate increased with temperature until 973 K and sample obtained by calcination at that temperature exhibited a rate of $200 \mu\text{mol h}^{-1}$, which was much higher than that of P-25 ($100 \mu\text{mol h}^{-1}$) as well as the mineralization system. This dependency suggests that balance of surface area and crystallinity, which control adsorptivity and e^- - h^+ recombination probability, respectively, is important in hydrogen evolution system.

3.3 Characterization and photocatalytic activities of brookite-type TiO_2

XRD pattern of the product is shown in Figure 7(a). All the XRD peaks of the product were assigned to brookite [21]. The crystallite size of this brookite sample was calculated to be 16 nm from the 121 diffraction peak using Scherrer equation. Due to the nano-crystalline property, this brookite sample had a large surface area of $78 \text{ m}^2\text{g}^{-1}$. In the previous paper [15], Raman spectroscopy and TEM observation revealed that the product consisted of agglomerates of brookite nano-crystals without contamination of other phases, anatase and rutile. In the TG curve of the product, weight loss was observed at the range from 473 to 773 K and total weight loss up to 1273 K was 6%. An exothermic peak was observed at 562 K in the DTA curve, which is attributed to combustion of organic moieties on the product. However, no DTA peak was observed in the high temperature region.

The brookite product was calcined at various temperatures and XRD patterns after calcination are shown in Figure 7(b)-(f). A very weak peak due to the rutile phase was observed after calcination at 823 K. Peaks of brookite became sharper after calcination at 973 K and formation of rutile TiO_2 was remarkable on calcination at 1173 K. The anatase form was not observed in XRD pattern of any calcined samples, indicating that brookite directly transformed to the rutile phase. These results of XRD were consistent with those of Raman spectroscopy [15]. Calcination temperature-dependency of physical properties of

the product is shown in Figure 8. Surface area of the sample gradually decreased with the elevation in calcination temperature while crystallite size increased, indicating that crystal growth of brookite occurred along with calcination and crystallinity of brookite sample was increased.

These brookite samples of various physical properties were platinized and then used for photocatalytic dehydrogenation of 2-propanol in aqueous suspensions. Effect of calcination on the H₂ evolution rate is shown in Figure 9. The rate increased with temperature until 973 K and sample obtained by calcination at that temperature exhibited a rate of 104 μmol h⁻¹, which was almost similar to that of P-25 (100 μmol h⁻¹). It should be noted that brookite-type TiO₂ exhibited high photocatalytic activity if it possesses adequate physical properties. Severer calcination decreased the rate as was observed in THyCA-TiO₂ (Figure 5). This same dependency suggests that balance of surface area and crystallinity, which control adsorptivity and e⁻-h⁺ recombination probability, respectively, is important in H₂ evolution system independent of the crystal structure of TiO₂.

3.4 Photocatalytic activity of WO₃ synthesized by hydrothermal method

Figure 10 shows XRD patterns of the powders obtained by HTT at various temperatures of H₂WO₄ solutions. Hydrated WO₃ (WO₃•0.33H₂O) [22] was obtained by HTT at 473 K (Figure 10(a)), while WO₃ with a monoclinic structure [23] was obtained at 523 K (WO₃-A) (Figure 10(b)), suggesting that WO₃ was produced via WO₃•0.33H₂O during HTT. For WO₃-A, the yield of WO₃ was estimated to be 94% on the basis of the molar amount of H₂WO₄ in the feed. Further increase in T_{HTT} up to 573 K and prolongation of HTT time at that temperature increased the crystallinity of WO₃ products (WO₃-B and -C, respectively) due to the higher solubility of tungsten species in water at higher T_{HTT} (Figures 10 (c) and (d)). As clearly shown in the XRD patterns, the intensities of 020, 200, 202, 220, 400, 402

diffraction peaks in these products increased with T_{HTT} up to 573 K, indicating that the growth of WO_3 crystallite proceeded toward a and b axes, especially the a axis, under HTT conditions at 573 K. SEM photographs of $\text{WO}_3 \cdot 0.33\text{H}_2\text{O}$, $\text{WO}_3\text{-A}$, $\text{WO}_3\text{-B}$ and $\text{WO}_3\text{-C}$ samples are shown in Figure 11. The $\text{WO}_3 \cdot 0.33\text{H}_2\text{O}$ sample consisted of agglomerates of fine particles, whereas $\text{WO}_3\text{-A}$ was composed of rectangular-shaped particles. This different morphology suggests that WO_3 was formed by a dissolution-recrystallization mechanism under HTT conditions. Higher T_{HTT} and longer HTT duration accelerated particle growth of WO_3 , and the length of the particle of WO_3 became longer, which was consistent with the results of XRD. Another feature of WO_3 particles observed in the SEM analyses is coagulation of particles by HTT of longer duration. The BET surface area (S_{BET}) of each sample is shown in Table 1. With elevation in T_{HTT} and prolongation of HTT time, S_{BET} of WO_3 decreased due to an increase in the size of primary WO_3 particles.

Figure 12 shows the time course of O_2 evolution from a suspension of $\text{WO}_3\text{-B}$ particles under UV-visible light irradiation. In this system, O_2 evolved linearly with irradiation time up to 20 min. The yields of O_2 and photodeposited Ag after 20-min irradiation was 23 and 89 μmol , respectively, and the $\text{Ag}/4\text{O}_2$ ratio was 0.97, indicating that O_2 evolution accompanying stoichiometric Ag deposition ($4\text{Ag}^+ + 2\text{H}_2\text{O} \rightarrow 4\text{Ag} + \text{O}_2 + 4\text{H}^+$) proceeds efficiently. The rate of O_2 evolution, i.e., the slope of the time-course curve, gradually decreased after 20 min. The pH of the suspension decreased with the above reaction producing H^+ , and the amount of Ag^+ adsorbed on photocatalyst particles decreased with lowering of pH [24,25], which accounts for the decrease in O_2 evolution. The activities of the present WO_3 samples were evaluated by the yields of O_2 and Ag after 20-min irradiation and are listed in Table 1. All WO_3 samples, including three commercial ones, tested in this study, exhibited activity, though the tungstite and $\text{WO}_3 \cdot 0.33\text{H}_2\text{O}$ samples showed negligible activity. Among the WO_3 samples listed in Table 1, the WO_3 samples of high crystallinity

prepared via IE-HTT showed higher activities than those of the commercial WO₃ samples; WO₃-B exhibited the highest activity. It has been pointed out that the crystallinity of TiO₂ controls the activity in photocatalytic O₂ evolution from an aqueous suspension of TiO₂ [19, 26]. The above-stated results clearly show that the same strategy of design can be applied to WO₃ photocatalyst for O₂ evolution. WO₃-C synthesized with a longer period possessed higher crystallinity and was expected to show higher activity than, for example, that of WO₃-B. However, this was not the case. As observed in SEM (Figure 11), WO₃-C particles, unlike WO₃-B particles, were strongly coagulated to give large secondary particles. It is known that grain boundaries of TiO₂ particles induce recombination of electron-hole pairs [27]. Coagulation of particles might produce crystal defects, at boundaries of WO₃ particles, acting as recombination centers of electron-hole pairs. WO₃-D prepared from solid H₂WO₄ by HTT showed a smaller O₂ yield than those of other HTT and commercial WO₃ samples. Crystallinity of the WO₃ powder might be insufficient for O₂ formation, which is supported by its relatively large S_{BET} (8.9 m²g⁻¹).

Photocatalytic activity was also examined with 2-h photoirradiation at a wavelength of > 420 nm using a cut-off filter. WO₃-B gave 12 μmol yield of O₂ under visible-light irradiation, though the apparent activity was much smaller than that with UV-visible irradiation due to the large decrease in the total number of photons irradiated to WO₃ particles. Degussa P-25, one of the most active TiO₂ photocatalysts, showed negligible O₂ evolution (0.3 μmol) due to the larger band gap energy (3.2 eV corresponding to ca. 390 nm).

4. Conclusion

Anatase and brookite-type TiO₂ and WO₃ samples were successfully synthesized by solvothormal technique. Physical properties of these semiconductors can be controlled by changing solvothormal condition and post-calcination temperature. These solvothormal

products exhibited higher or similar activities than commercial active Degussa P-25 in several photocatalytic reaction systems.

Acknowledgement

This work was partly supported by grants-in-aid from the Ministry of Education, Science, Sports, and Culture of Japan (09750861, 09218202, 09044114, and Priority Areas 417).

References

- [1] T. Wakanabe, A. Kitamura, E. Kojima, C. Nakayama, K. Hashimoto and A. Fujishima, p. 747, in: Photocatalytic purification and treatment of water and air, eds. D. E. Ollis and H. Al-Ekabi, Elsevier, 1993.
- [2] M. A. Fox and M. T. Dulay, *Chem. Rev.* 93 (1993) 341.
- [3] M. R. Hoffmann, S. T. Martin, W. Choi and D. W. Bahnemann, *Chem. Rev.* 95 (1995) 69.
- [4] T. Ibusuki and K. Takeuchi, *J. Mol. Catal.* 88 (1994) 93.
- [5] B. Ohtani and S.-i. Nishimoto, *J. Phys. Chem.* 97 (1993) 920.
- [6] M. Kiyama, T. Akita, Y. Tsutsumi and T. Takada, *Chem. Lett.* 1972, 21.
- [7] T. Mitsuhashi and M. Watanabe, *Mineralogical Journal* 9 (1978) 236.
- [8] B. Ohtani, J.-i. Handa, S.-i. Nishimoto and T. Kagiya, *Chem. Phys. Lett.* 120 (1985) 292.
- [9] J. R. Darwent and A. Mills, *J. Chem. Soc., Faraday Trans.*, 2 78 (1982) 359.
- [10] W. Erbs, J. Desilvestro, E. Borgarello and M. Grätzel, *J. Phys. Chem.* 88 (1984) 4001.
- [11] K. Sayama and H. Arakawa, *J. Phys. Chem.* 97 (1993) 531.
- [12] T. Ohno, F. Tanigawa, K. Fujihara, S. Izumi and M. Matsumura, *J. Photochem. Photobiol. A: Chem.* 118 (1998) 41.
- [13] K. Byrappa and M. Yoshimura, *Handbook of Hydrothermal Technology*, Noyes, 2001.
- [14] M. Inoue, K. Kitamura, H. Tanino, H. Nakayama and T. Inui, *Clays Clay Miner.* 37 (1989) 71.
- [15] H. Kominami, M. Kohno and Y. Kera, *J. Mater. Chem.* 10 (2000) 1151.
- [16] B. Ohtani, M. Masuoka, T. Atsumi, S.-i. Nishimoto and T. Kagiya, *Chem. Express* 3 (1988) 319.
- [17] H. Kominami, J.-i. Kato, M. Kohno, Y. Kera and B. Ohtani, *Chem. Lett.* (1996) 1051.
- [18] S.-i. Nishimoto, B. Ohtani and T. Kagiya, *J. Chem. Soc., Faraday Trans.* 1 81 (1985) 61.

- [19] H. Kominami, S.-y. Murakami, Y. Kera and B. Ohtani, *Catal. Lett.* 56 (1998) 125.
- [20] JCPDS card No. 21-1272.
- [21] JCPDS card No. 29-1360
- [22] JCPDS card No. 35-0270
- [23] JCPDS card No. 43-1035
- [24] B. Ohtani and S.-i. Nishimoto, *J. Phys. Chem.* 1993, **97**, 920.
- [25] B. Ohtani, Y. Okugawa, S.-i. Nishimoto and T. Kagiya, *J. Phys. Chem.* 1987, **91**, 3550.
- [26] H. Kominami, T. Matsuura, K. Iwai, B. Ohtani, S.-i. Nishimoto and Y. Kera, *Chem. Lett.*, 1995, 693.
- [27] P. T. Landsberg, *Recombination in Semiconductors*, Cambridge University Press, Cambridge (1991), p. 208.

Figure captions

Figure 1 Reaction apparatus

Figure 2 XRD patterns of (a) TiO_2 prepared by the alcohothermal treatment of titanium n-butoxide in 2-butanol at 573 K, and (b), (c), and (d) the samples obtained by calcination of (a) at 823, 973 and 1173 K, respectively.

Figure 3 A TEM photograph of TiO_2 prepared by the alcohothermal treatment of titanium n-butoxide in 2-butanol at 573 K

Figure 4 Effect of calcination on surface area and crystallite size of THyCA- TiO_2 .

Figure 5 Effect of calcination on the CO_2 evolution rate of THyCA- TiO_2 in photocatalytic mineralization of acetic acid.

Figure 6 Effect of calcination on the H_2 evolution rate of platinumized THyCA- TiO_2 in photocatalytic dehydrogenation of 2-propanol in aqueous suspension.

Figure 7 XRD patterns of (a) TiO_2 prepared by the solvothelmal treatment of $\text{TiO}(\text{acac})_2$ in EG- H_2O in the presence of sodium acetate at 573 K, and (b), (c), (d), (e) and (f) the samples obtained by calcination of (a) at 623, 823, 973, 1073 and 1173 K, respectively.

Figure 8 Effect of calcination on surface area and crystallite size of brookite-type TiO_2 .

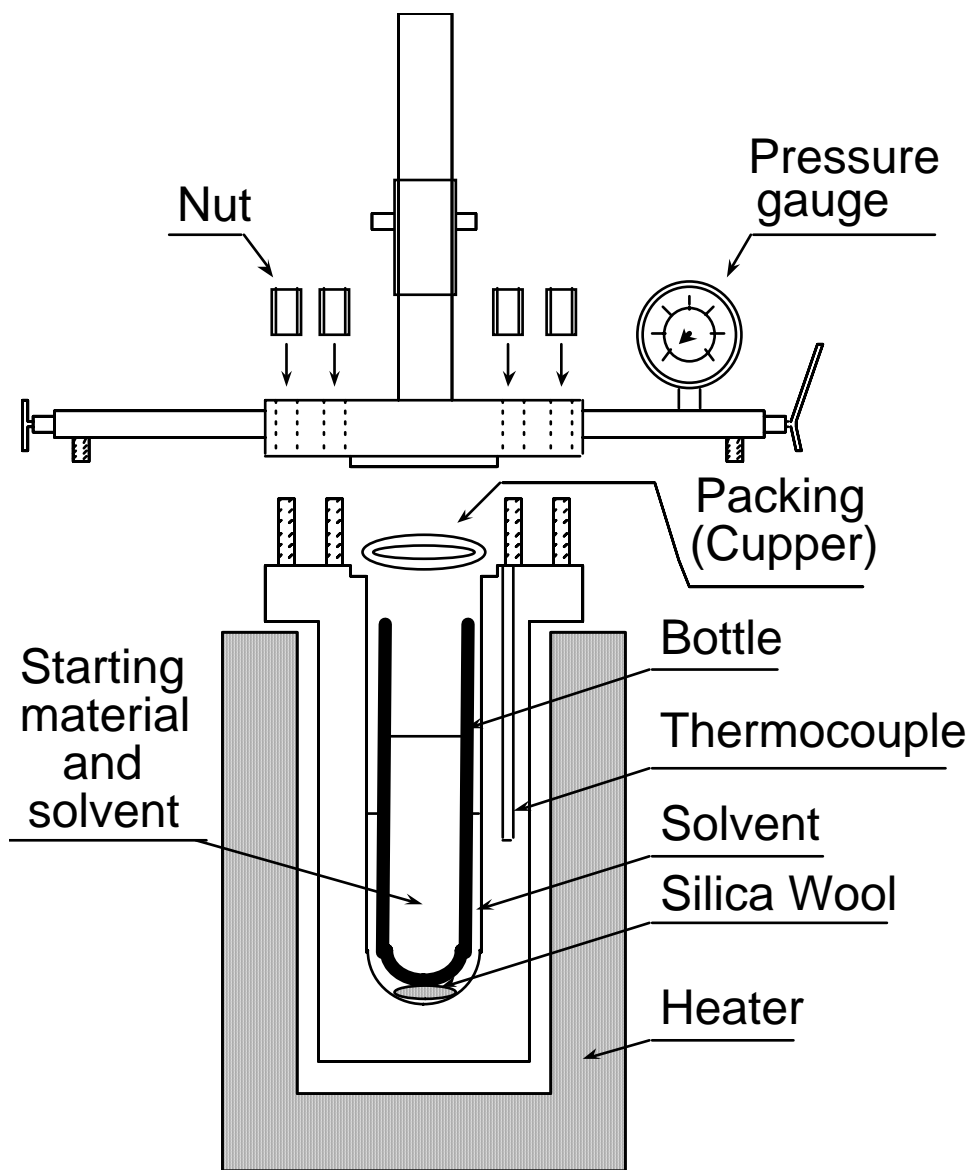
Figure 9 Effect of calcination on the H_2 evolution rate of platinumized brookite- TiO_2 in photocatalytic dehydrogenation of 2-propanol in aqueous suspension.

Figure 10 XRD patterns of the compounds obtained by HTT of an H_2WO_4 solution at (a) 473 K for 2 h, (b) 523 K for 2 h (WO_3 -A), (c) 573 K for 2 h (WO_3 -B), and (d) 573 K for 8 h (WO_3 -C).

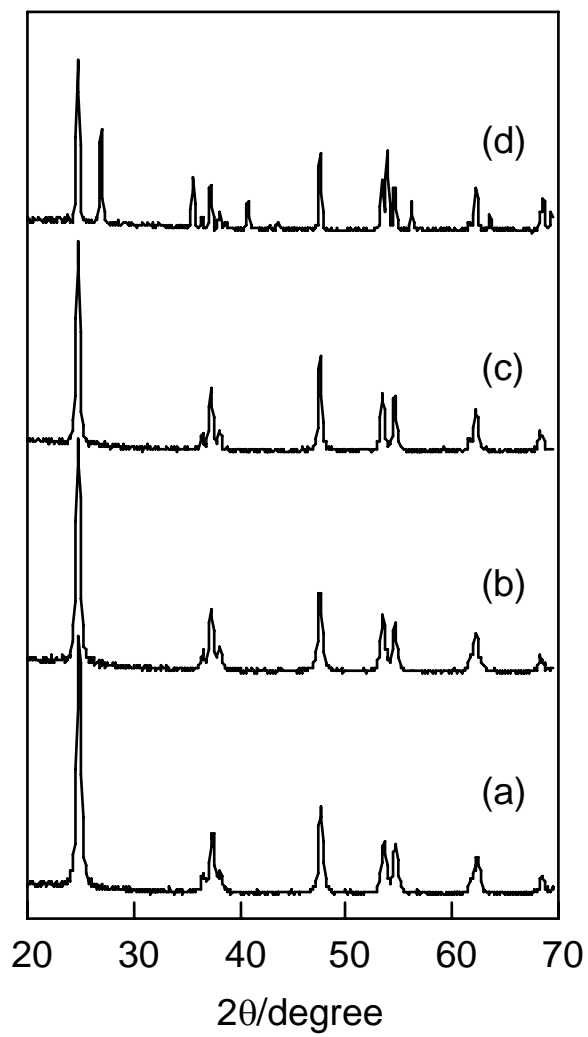
Figure 11 SEM photographs of the compounds whose XRD patterns are shown in Figure 10.

Figure 12 Time course of O_2 evolution from Ag_2SO_4 in an aqueous suspension of

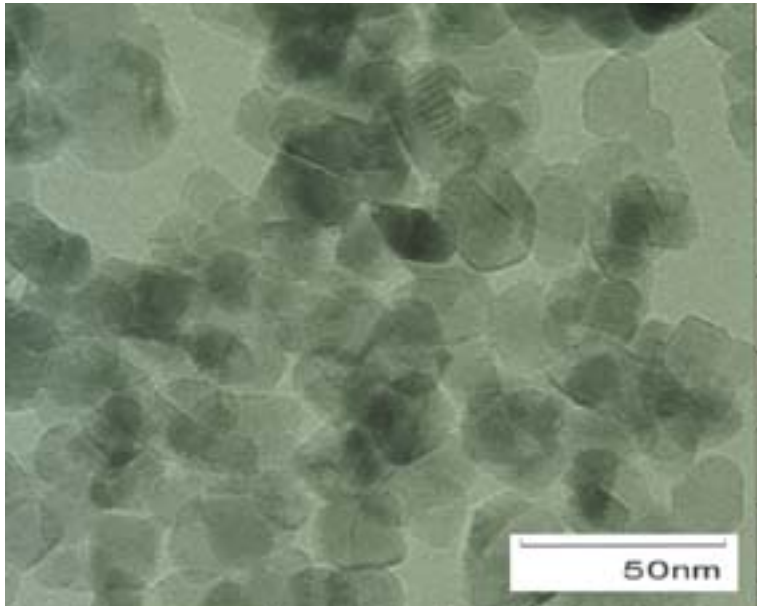
WO₃-B under UV-visible light irradiation.



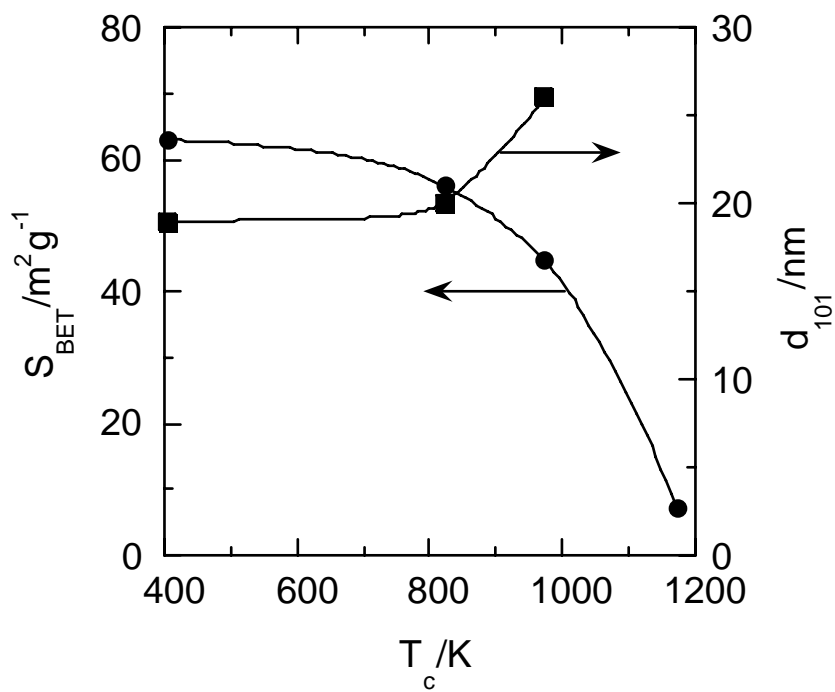
Kominami et al., Fig. 1



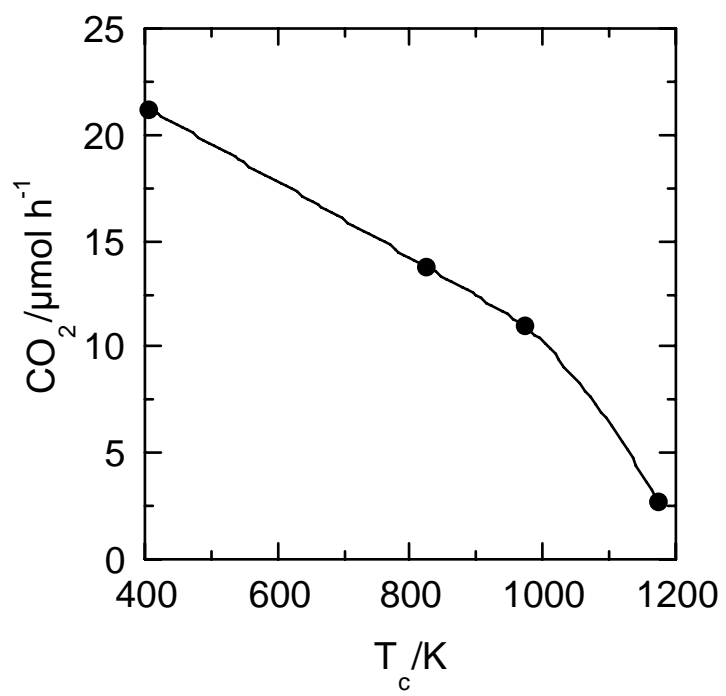
Kominami et al., Fig. 2



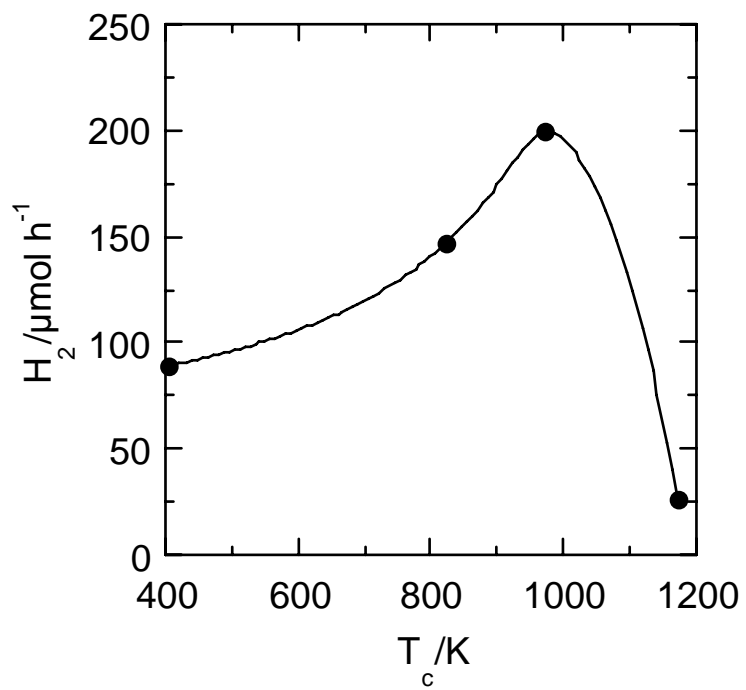
Kominami et al., Fig. 3



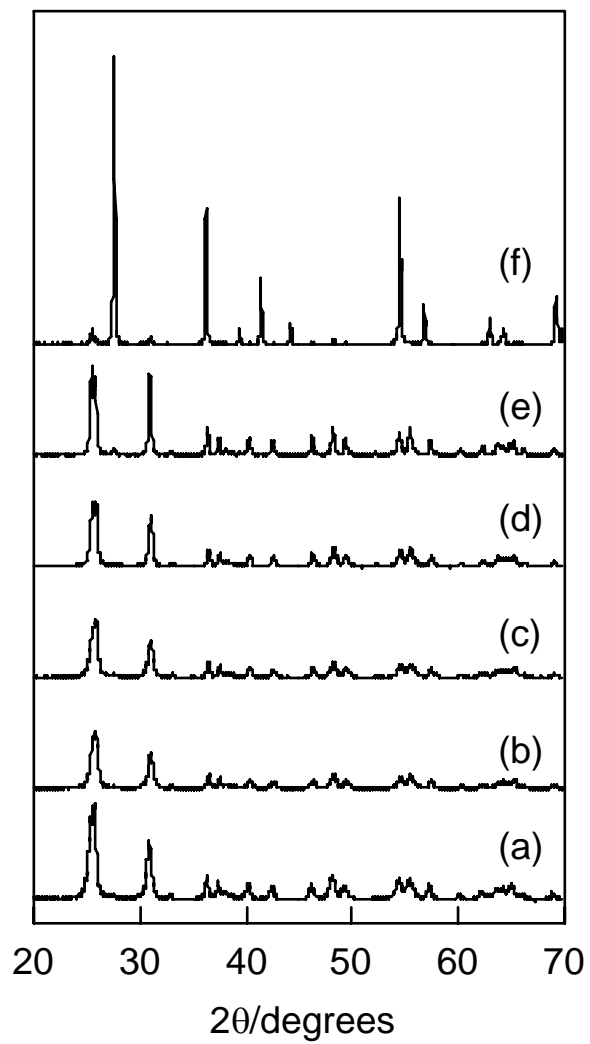
Kominami et al., Fig. 4



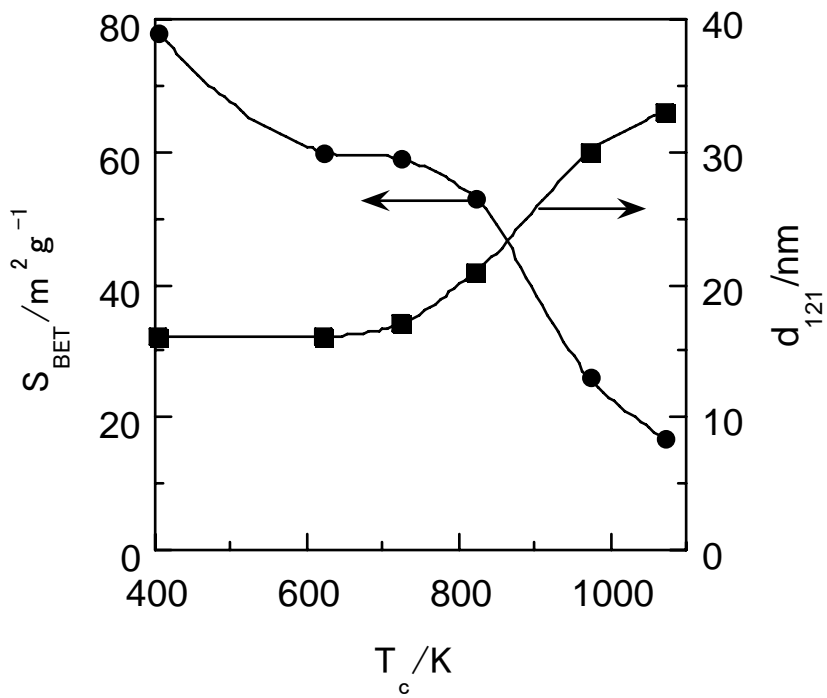
Kominami et al., Fig. 5



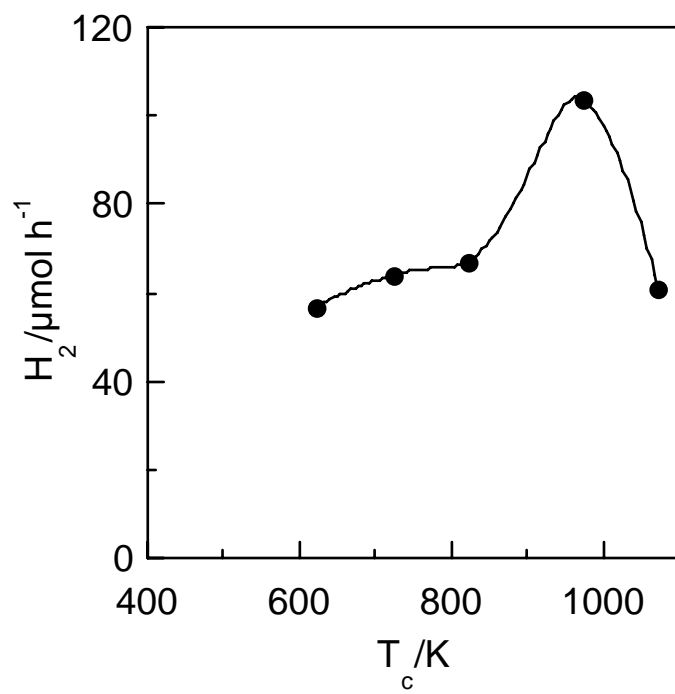
Kominami et al., Fig. 6



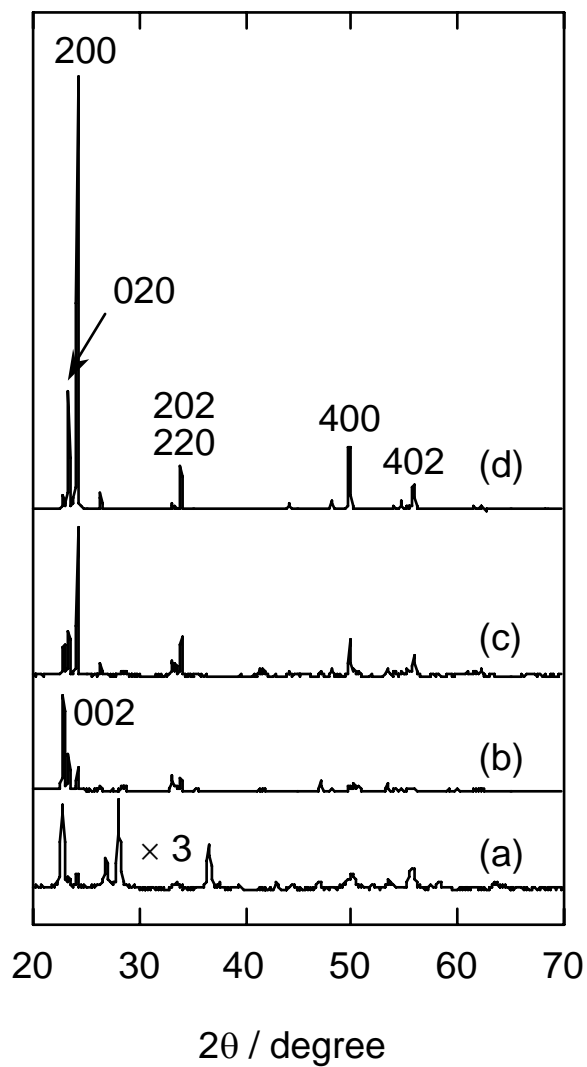
Kominami et al., Fig. 7



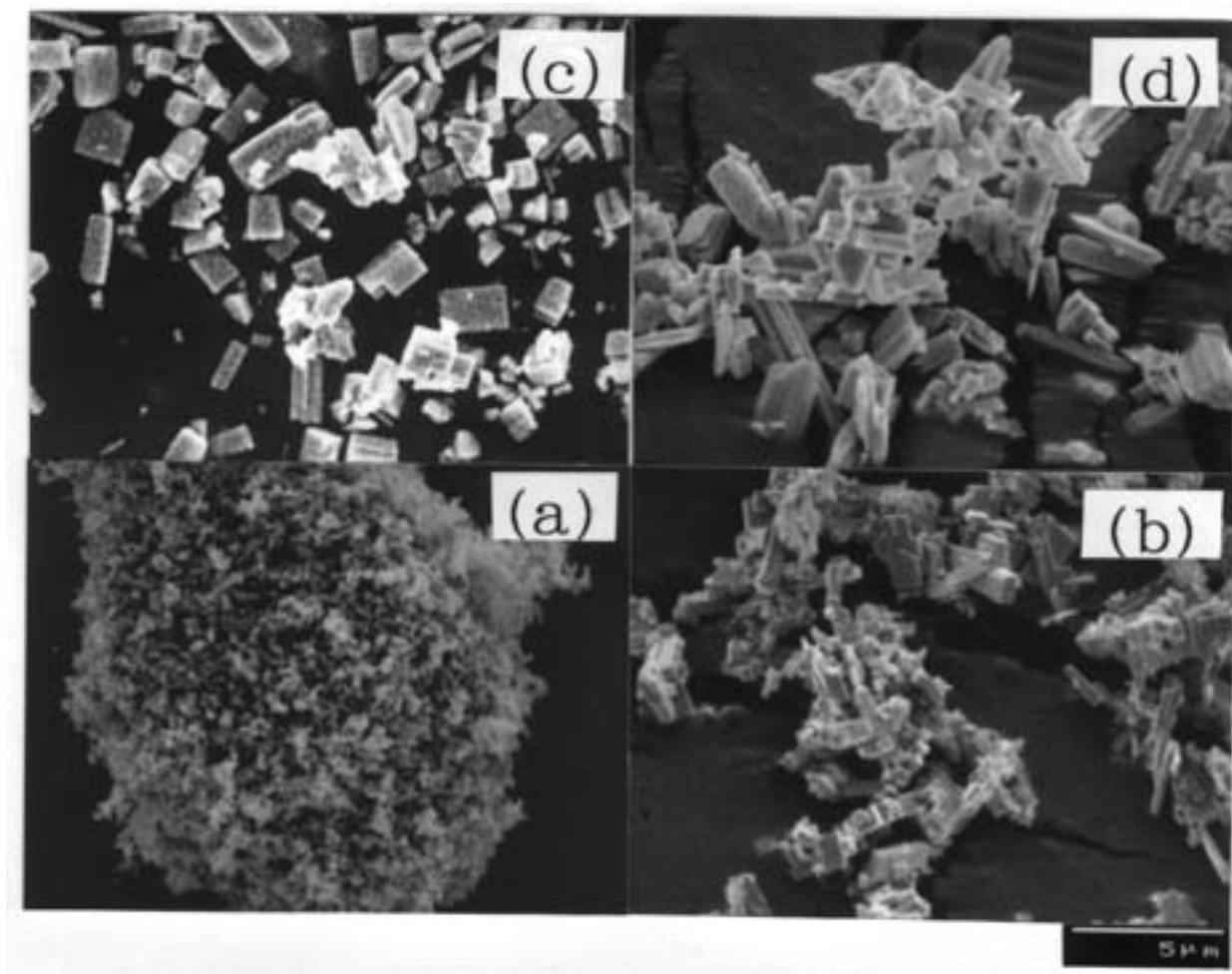
Kominami et al., Fig. 8



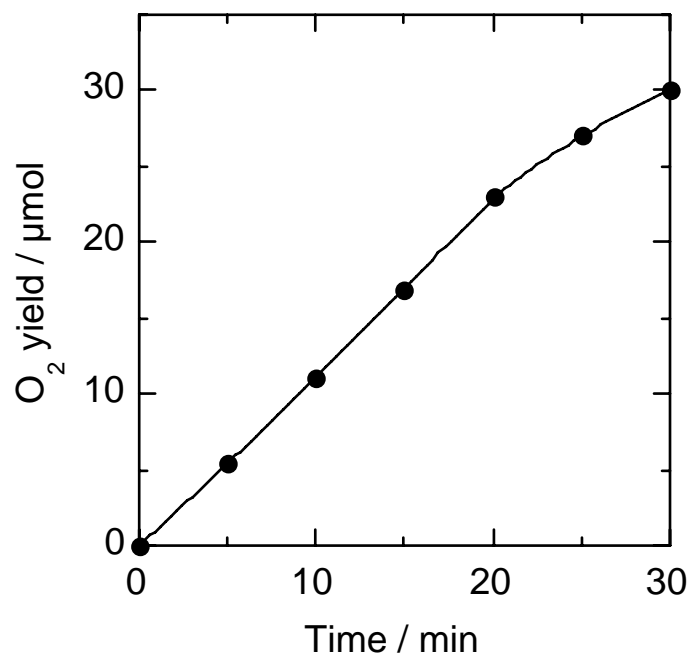
Kominami et al., Fig. 9



Kominami et al., Fig. 10



Kominami et al., Fig. 11



Kominami et al., Fig. 12

Table 1Photocatalytic activity (20-min irradiation) of HTT-WO₃ products prepared from various starting materials

sample	H ₂ WO ₄ material	T _{HTT} ^a / K	t _{HTT} ^a / h	phase	S _{BET} / m ² g ⁻¹	O ₂ / μmol	Ag / μmol	Ag / 4O ₂
WO ₃ •0.33H ₂ O	solution ^b	473	2	orthorhombic	18	1.9	8.2	1.1
WO ₃ -A	solution ^b	523	2	monoclinic	14	9.6	36	0.94
WO ₃ -B	solution ^b	573	2	monoclinic	1.7	23	89	0.97
WO ₃ -C	solution ^b	573	8	monoclinic	0.6	15	58	0.97
WO ₃ -D	solid ^c	573	2	monoclinic	8.9	3.0	13	1.1
WO ₃ -E ^d				monoclinic	3.0	11	47	1.1
WO ₃ -F ^e				monoclinic	3.1	9.8	41	1.0
WO ₃ -G ^f				monoclinic	5.0	6.5	25	0.96
(P-25 TiO ₂) ^g				anatase, rutile	50	4.3	19	1.1

^aHydrothermal treatment was carried out at T_{HTT} for t_{HTT}.^b0.19 mol dm⁻³, 75 cm³^cSupplied as tungstic acid from Kanto Chemicals.^dHigh Purity Chemicals (99.99% purity).^eKishida Chemicals (99.9% purity).^fKanto Chemicals (99.5 % purity).^gDegussa.